Mechatronics and buoyancy implementation of robotic fish swimming with modular fin mechanisms

K H Low
School of Mechanical and Aerospace Engineering, Nanyang Technological University, Singapore, 639798, Singapore.
email: mkhlow@ntu.edu.sg

The manuscript was received on 3 April 2006 and was accepted after revision for publication on 1 November 2006.

DOI: 10.1243/09596518JSCE276

Abstract: This paper presents an underwater vehicle mimicking the undulating fins of fish. To mimic the actual flexible fins of real fish, a fin-like mechanism is modelled with a series of connecting linkages. By virtue of a specially designed strip, each link is able to turn and slide with respect to the adjacent link. The driving linkages are used to form a mechanical fin consisting of several fin segments, which are able to produce undulations similar to those produced by the actual fins. Owing to the modular design and the flexible structure of the mechanical fin, it is possible to model different types of fin and to construct various biomimetic robots of fish swimming by fin undulations. On the other hand, a buoyancy tank has been designed and attached to the modular fin mechanisms for the complete fish swimming capability. The workspace of the fin mechanism is derived and applied in locomotion implementation. The mechatronics design and locomotion control of the integrated robotic fish are presented. Some qualitative and workspace observations by experiments with the robotic fish are also shown and discussed.

Keywords: biomimetic, robotic fish, modular fin mechanism, undulating-fin motion, buoyancy tank

1 INTRODUCTION

Marine propulsion and manoeuvring have a long history of development and have already reached a level of maturity. This level is in some aspects satisfactory and in other aspects, particularly for transient motion, rather limiting [**1**]. Fast fish and cetaceans, on the other hand, move with great agility in water. They propel themselves through rhythmic unsteady motions of their body, fins, and tail; they offer a different paradigm of locomotion from that conventionally used in man-made vehicles.

Recently, researchers and scientists have been more vocal than in the past in promoting an awareness to preserve environment [**2**]. One of their main concerns is the sustainability of underwater ecology, especially marine environment, which is deteriorating owing to the extensive use of propellers and has recently gained public and government attention.

Novel propulsion ideas have emerged recently as progress in robotics, new materials, and actuators have become available. Propulsors and vehicles that emulate the motion of fish have been developed for technological application, using state-of-the-art technology, robotics, and an understanding of how fish swim. On the other hand, fin-based propulsion systems perform well for both high-speed cruising and high manoeuvrability in fish, making them good models for propulsors of underwater vehicles.

Biomimetics is an emerging field, using principles from living organisms to derive man-made mechanisms and machines that are capable of emulating the performance of animals [**3**]. In the field of underwater research, an undulating-fin robot offers exceptional advantage over a propeller in preserving an undisturbed condition of its surroundings for data acquisition and task execution. Military and defence are most important areas where biomimetics finds its significant role in ensuring safe waters; the undulating-fin robot might be undetected when swimming with a school of fish and therefore may act as a spy.

In hydrodynamics, highly accurate robotic mechanisms are used to measure the power needed and

forces generated, as well as to visualize the flow around their external skin structure [**4**]. Kato [**5**] and Read [**6**] studied the use of fins in small underwater vehicles for hovering and low-speed manoeuvring.

Barrett *et al.* [**7**] used a laboratory robot to study the effect of a fish-like body motion on the axial and transverse forces and hence the power required for swimming. The development of their high-precision multilink robotic mechanism, which can emulate very closely the swimming of the tuna [**8–10**], overcomes the difficulties associated with working with live fish because it allows the acquisition of detailed measurements of the forces on an actively controlled flexible body.

As fish are impressive swimmers in many ways, it is hoped that submersible robots that swim like fish might be superior to submersibles using propellers. Fish-like robots are expected to be quieter, more manoeuvrable and possibly more energy efficient. In addition, each species has its own unique and optimum way of interacting with its environment, which then dictates the species' body shape, body size, and the way that it propels itself. This has led to the biological study and biomimetics development and study of robotic fish by many researchers [**11–15**].

To focus mainly on the biomimetic design of actual flexible fins, a robotic fish with a specially designed modular fin mechanism and buoyancy body is constructed. The fin mechanism provides the function of a flexible membrane by using a slider. The modular concept enables various biomimetic robots of fish swimming by fin undulations to be constructed. The locomotion implementation and buoyancy control of the robotic fish are also presented and discussed. Finally, the preliminary testing of the robotic fish is discussed with the results presented.

2 MECHANICAL FIN DESIGN

2.1 Fish swimming modes

Breder [**16**] proposed two swimming modes of fish based on the propulsive structure used: *body and/or caudal-fin* (BCF) locomotion and *median and/or paired-fin* (MPF) locomotion. Fish under BCF locomotion generate thrust by bending their body into a backward-moving propulsive wave that extends to its caudal fin, which is shown in Fig. 1. BCF locomotion is further classified into five subcategories, based on the degree of body undulation, as shown in Fig. 2. Similarly, MPF locomotion is classified into several subcategories, based on the fins used as the propulsive structure, as shown in Fig. 2. However, the present interest is in fish whose fins undulate roughly parallel to the direction of motion. *Rajiform*, *amiiform*, and *gymnotiform* are those undulating-fin subcategories considered in this research, as shown in Fig. 3.

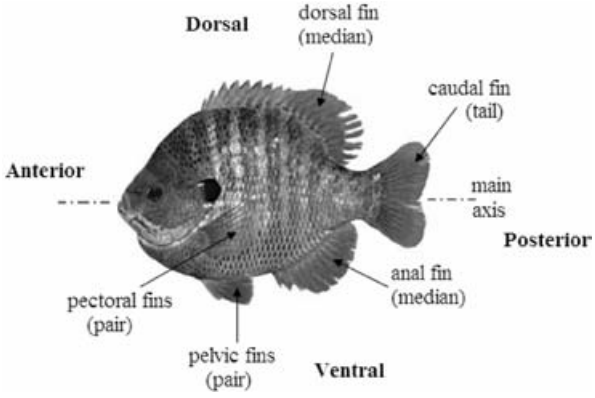

Fig. 1 Fish morphology to identify fins in different swimming modes (modified from reference [**17**])

2.2 Design of the fin rays

An interesting swimming gait is found in rajiform swimmers, such as the stingray. Thrust is produced by large undulations along pectoral fins, which span from the anterior to the posterior of the fish. The amplitude envelope of the undulations increases from the anterior part to the fin apex and decreases towards the posterior.

Kier and Thompson [**19**] suggested that the fins of the stingray are supported by a three-dimensional array of muscle. The designs of actuators, both linear and rotary, are unable to model the complex musculature of the fins of the stingray.

Despite the complexity of the actual musculature, the fins of the stingray exhibit much the same undulations as that displayed by the fins of the ray-finned fish with an undulatory swimming mode.

Flexible materials such as plastic sheet, cloth, and thin rubber sheet are conventionally considered to model a membrane and to connect all the cranks. The main disadvantage of such materials when used in a flexible membrane is that they assume any unpredictable shape, which can disturb the water flow and movement of the fin. Thin rubber sheet may be an ideal material. However, the rubber is required to elongate, and extra power is needed therefore in addition to the power required to push water. To overcome this situation, the cranks must be closely spaced, such as found in fish, and therefore many actuators are required in order to have at least one smooth wavelength in an undulating fin [**7**].

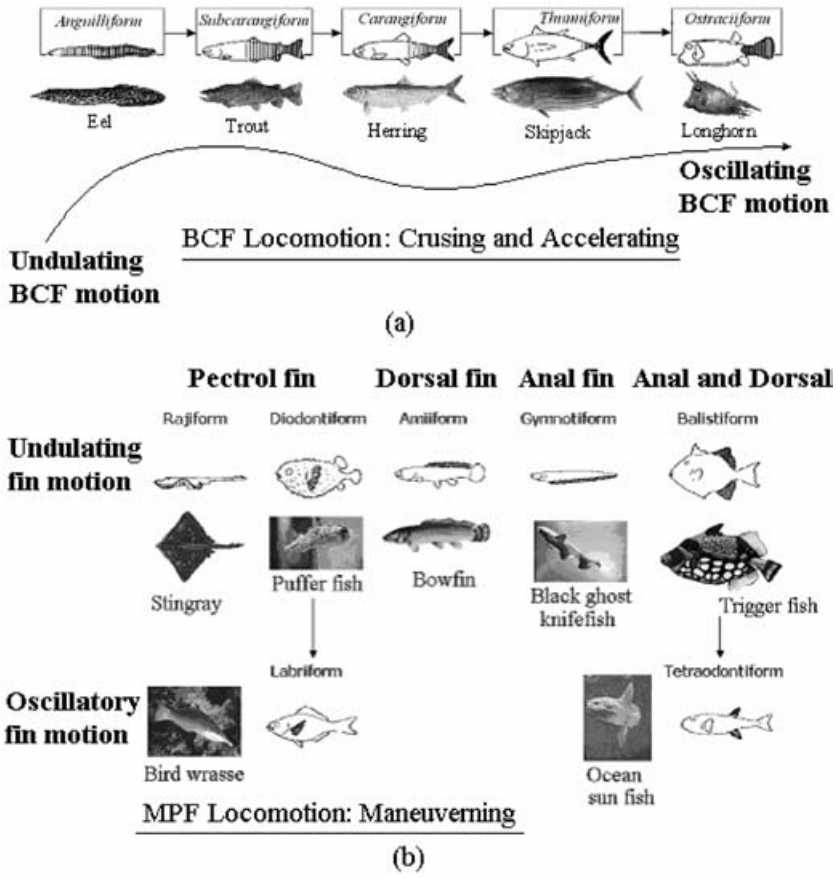

Fig. 2 Classification of swimming modes (modified from references [**17**] and [**18**])

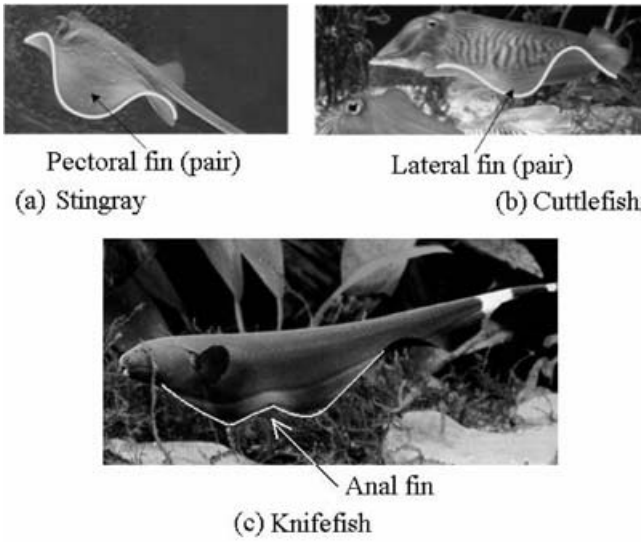

Fig. 3 Fish swimming with undulating fins

In order to simplify our modelling, the fin of the stingray is divided into many segments such that the fin looks similar to that of the ray-finned fish. From the mechanical point of view, the fins of the stingray can also be supported by a rigid structure such as fin rays so as to perform undulatory movements. Figure 4 shows a fin diagram of any fish, including that of the stingray, performing undulations. The universal joint (U) is one possible joint that permits two-degrees-of-freedom movements at the base of each fin ray. The fin segments can also model dorsal and median fins, as shown in Fig. 1.

2.3 Design of the flexible membrane

At the present stage, the mechanical modelling of undulating fins, which includes those of the stingray and ray-finned fish, is simplified to one degree of freedom from originally two degrees of freedom at

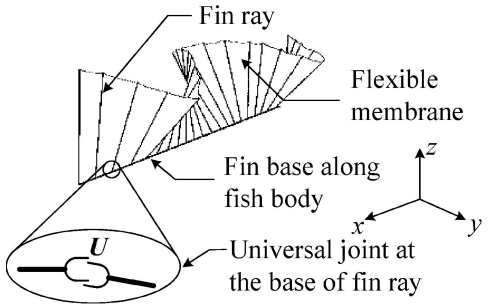

Fig. 4 Fin diagram of the ray-finned fish

the base of each fin ray. As shown in Fig. 5, a servomotor serves as a muscle producing one degree of freedom at the base of each ray. A crank is next attached to the servomotor to function as a fin ray. In order for the fin to exhibit undulations similar to that of any undulating fin, each servomotor is programmed so that the crank attached to the servomotor oscillates based on a specified sinusoidal function.

The developed mechanism will enable the flexible membrane to maintain a straight line between two cranks and at the same time to be extendible, since the distance between two cranks changes as they oscillate. Figure 5(b) shows the kinematic diagram of a linkage representing two cranks AB and ED and a membrane BD. The linkage in Fig. 5(b) possesses two degrees of freedom since points A and E are each driven by a servomotor. Details of the designed mechanisms and the fin locomotion can be found in references [**20**] to [**22**].

As shown in Fig. 6, the multisegment fin mechanism is able to model any sinusoidal waveform

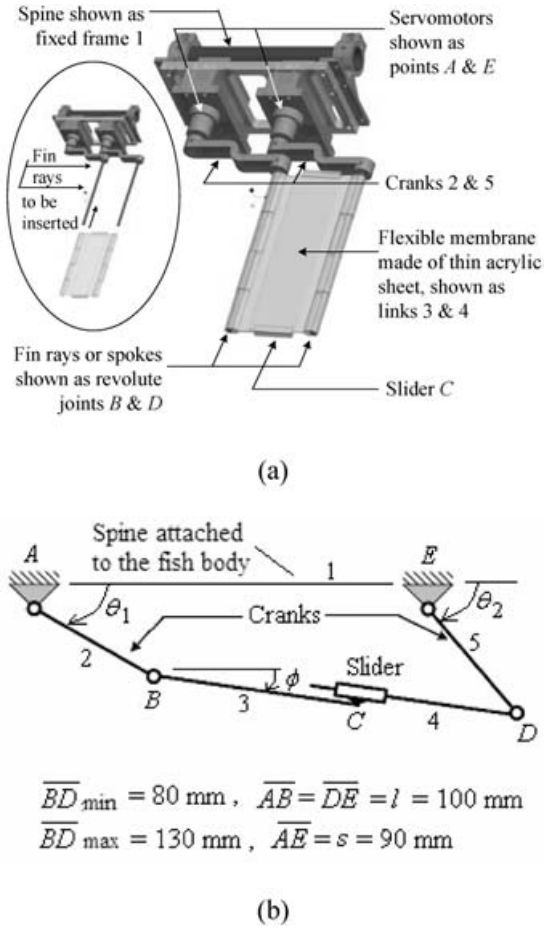

Fig. 5 A segment of a fin pair: (a) computer assisted design model; (b) kinematic diagram

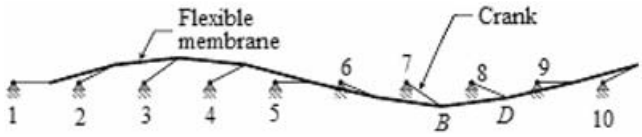

Fig. 6 Arbitrary sinusoidal waveforms generated by a series of cranks connected by straight lines (e.g. link BD with changing length)

discretely by a series of straight lines; one straight line joins two points on a sinusoidal curve with varying waves. Figure 7 illustrates that a higher number of the waves (or cycles) can be generated by the increasing number of servomotors.

2.4 Workspace of the mechanism

The analysis of the fin is simplified to one fin segment, which is controlled by two servomotors A and E, whose angular displacements with respect to the horizontal axis are specified by θ_1 and θ_2 respectively, as shown in Fig. 5. Note that the linkage in the figure has two degrees of freedom and BD is a link whose length varies according to the orientations of cranks AB and DE.

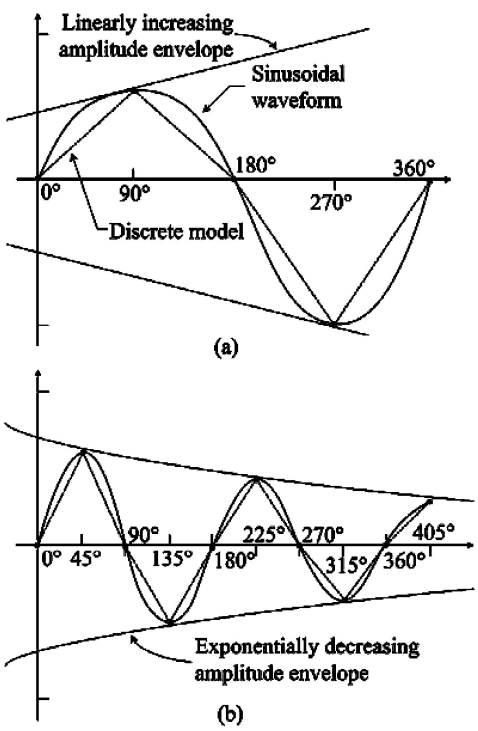

Fig. 7 Discrete model of sinusoidal waveforms developed by series of straight lines joining two points in every (a) 90° (i.e. five motors) and (b) 45° (i.e. ten motors)

The position vector and the length of link BD are

$$\boldsymbol{P}_{\mathrm{BD}} = \boldsymbol{P}_{\mathrm{B}} - \boldsymbol{P}_{\mathrm{D}}$$

$$= l(\cos\theta_1 \boldsymbol{i} + \sin\theta_1 \boldsymbol{j}) - l\left[\left(\frac{s}{l} + \cos\theta_2\right)\boldsymbol{i} + \sin\theta_2 \boldsymbol{j}\right]$$

$$\|\mathrm{BD}\| = \sqrt{\left[l\left(\frac{s}{l} + \cos\theta_2 - \cos\theta_1\right)\right]^2 + [l(\sin\theta_2 - \sin\theta_1)]^2} \tag{1}$$

respectively and its orientation with respect to the horizontal line is

$$\phi = \tan^{-1}\left(\frac{\sin\theta_2 - \sin\theta_1}{s/l + \cos\theta_2 - \cos\theta_1}\right) \tag{2}$$

Consider the fin segment in Fig. 5 moving at a specified speed and the two servomotors performing *harmonic oscillations* according to the functions

$$\theta_1 = a\sin\alpha \quad \text{and} \quad \theta_2 = b\sin(\alpha + \beta) \tag{3}$$

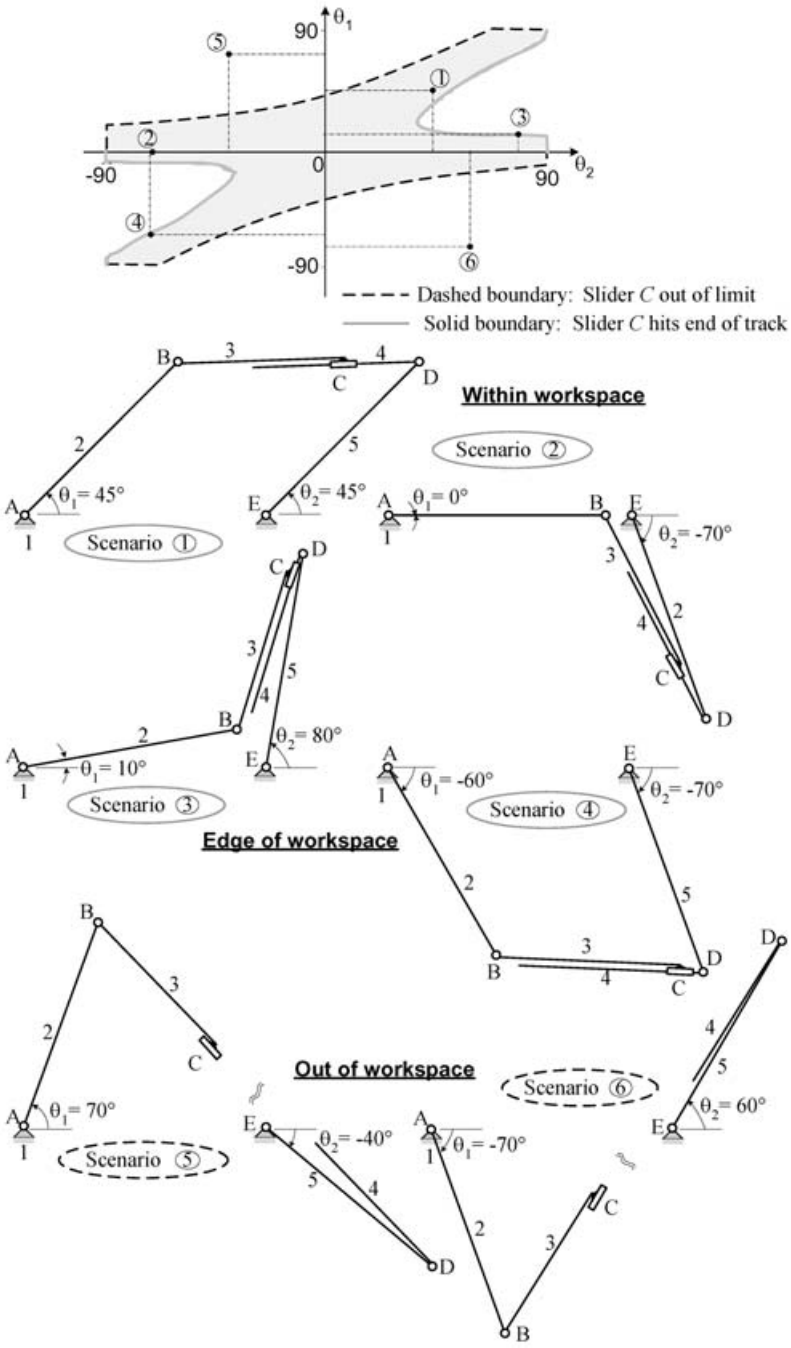

Fig. 8 Workspace of the single fin segment, shown by the grey area and the black boundaries which signify the slider limitations

where a and b are the maximum angular oscillations of θ_1 and θ_2 respectively, while β is the phase difference between θ_1 and θ_2.

An important advantage possessed by the mechanism shown in Fig. 5 is that it will perform a predictable shape. Points B and D will always join with a straight line. The mechanism design allows the flexible membrane, represented by links 3 and 4 and the slider C, to contract to a minimum length of 80 mm and to be extended up to 130 mm. This therefore poses a certain constraint in the workspace of the mechanism, as shown by the grey area in Fig. 8. There are two scenarios that will happen because of the mechanical limitation.

Scenario 1. The slider C will hit the end of the track when the mechanism tries to contract to a length less than 80 mm.

Scenario 2. The slider C will run off the track when the mechanism tries to extend beyond 130 mm.

Scenarios 1 and 2 in Fig. 8 are then the boundaries of the workspace, which are shown as a grey curve and a dashed black curve respectively.

3 FIN TRAJECTORY PLANNING AND CONTROL

Based on the design methodology described in section 2, a finned propulsion system has been designed and is able to model undulating fins of underwater creatures, such as the stingray, knifefish, and cuttlefish, in order to investigate various swimming methods. The locomotion implementation of the undulating fin is discussed next.

As an example, a robotic stingray fin with 20 servomotors shown in Fig. 9 (ten servomotors proposed in each side; another number of servomotors is possible) is controlled by six microcontrollers, divided into three levels of communication for efficient programming.

As shown in Fig. 10, there are two microcontrollers in level 1 acting as a data miner and a clock. The data miner is used to obtain the user input command, and the clock is used to synchronize the processes of all microcontrollers. A 25 ms clock time was specified by the servomotors as the maximum time to process one cycle of instructions.

The computations in level 2 are made in 15 ms, and the data are next transferred to a corresponding microcontroller in level 3. The technique is the so-called parallel processing technique because all microcontrollers are carrying out different tasks that are all synchronized by a clock.

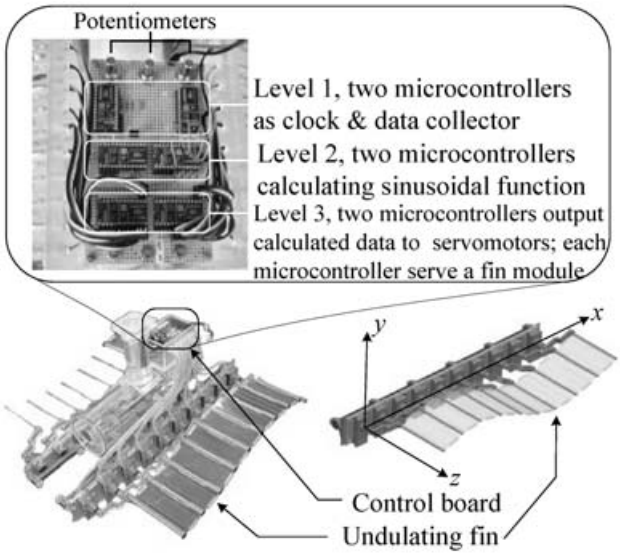

Fig. 9 Layout of the fin control board consisting of six microcontrollers, arranged in three levels of communications, and three potentiometers that alter some parameters of the undulating fin

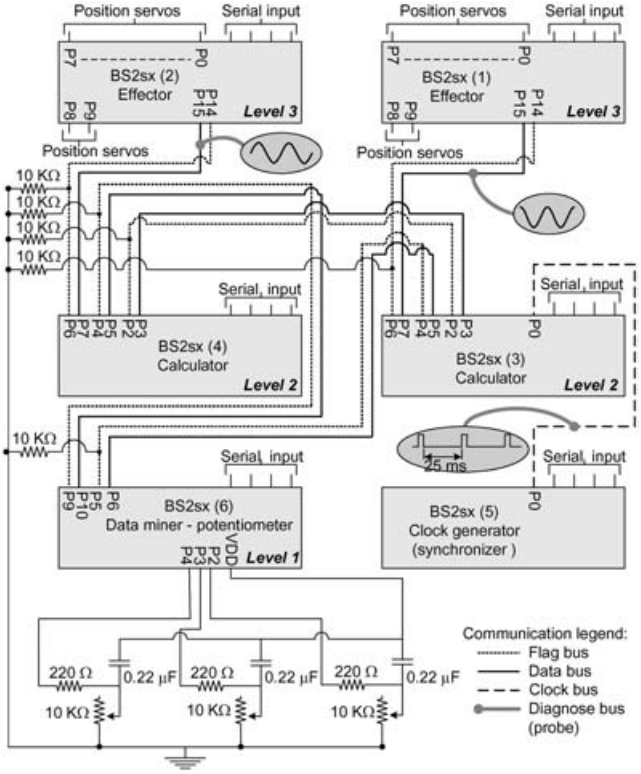

Fig. 10 Circuitry for the fin locomotion control

The multisegment fin can accommodate various amplitude envelopes, motor frequencies, and wavelengths. To fit the programming purpose, the equation

$$\theta_n(t) = g_n \sin[2\pi\alpha t + (n-1)\beta] \tag{4}$$

whose parameters are provided in Fig. 11, is used. The value n in equation (4) is used to indicate the number of servomotors, and the equation can therefore be seen as a discrete model of an undulating fin by a specified number of servomotors (see Fig. 7). Figure 12 illustrates the relationship between the servomotor frequency and number and the servomotor angles.

The amplitude envelope g_n defines the oscillation path of the respective crank of the servomotors, which can be mapped into one circular path. Other amplitude envelopes, such as the linearly increasing amplitude envelope, can be described as

$$g_1 = c, \quad g_2 = 2g_1, \quad g_3 = 3g_1, \ldots, g_n = ng_1 \tag{5}$$

where c is a constant. Note that the amplitude envelope has n circular paths for different diameters depending on the specified oscillation amplitude of each crank.

3.1 Limit of the workspace

After the desired amplitude envelope and phase difference have been determined, it is important to check whether the undulating-fin mechanisms will encounter any mechanical limitations in the workspace. For the mechanisms to work properly, the angular positions of all fin segments must lay in the workspace defined in Fig. 8. By virtue of equation (1), the workspace of the fin segments to generate such positions, with different servomotors and times, is shown in Fig. 13 with three β and two α. It is obvious that the wave number increases for a higher phase difference, given the same servomotor number. On the other hand, the oscillation wave of a given motor increases if the motor rotates more quickly. Figures 14 and 15 show trajectories traced at various β and the limiting ranges.

4 BUOYANCY TANK

An organ known as the swim bladder [**23**] allows the fish to adjust its density quickly, relative to its surroundings, by changing the volume of the bladder. Submarines use ballast tanks, which are tanks flooded with water to enable the submarine to dive, surface, and maintain depth underwater.

Some underwater robots employ piston mechanisms to model the ballast of a submarine. Another

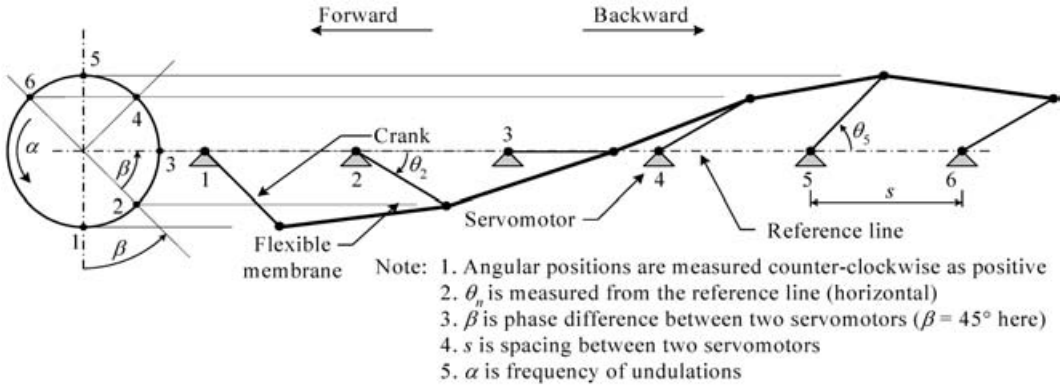

Fig. 11 Parameters designation for the undulating fin

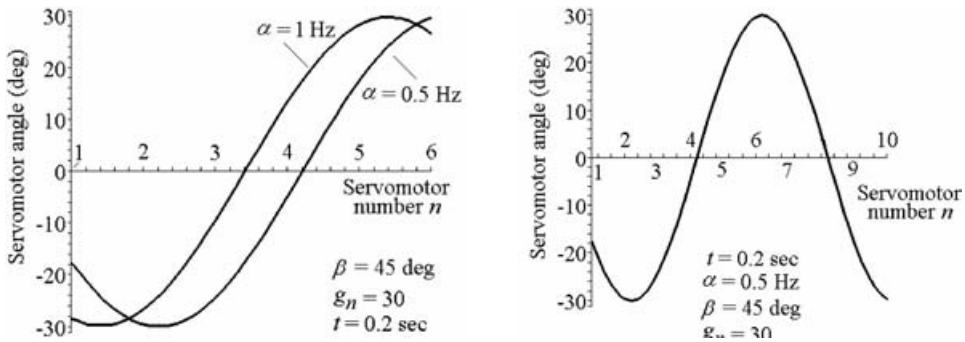

Fig. 12 Servomotor angles: (a) different rotations with $n = 6$; (b) the result with $n = 10$

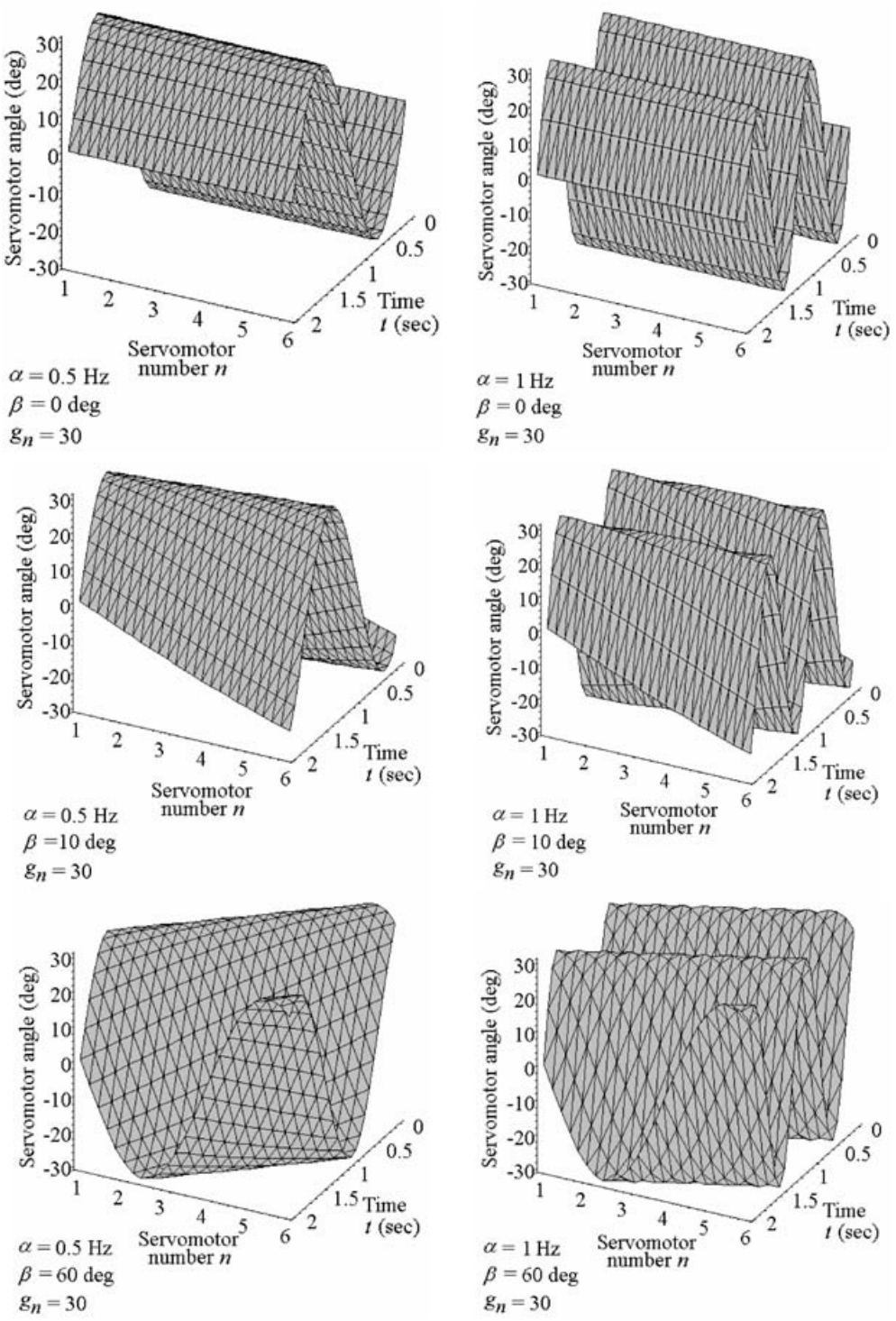

Fig. 13 Positions traced by the undulating fin at various differences β

method to control the depth of a vessel is by using propeller(s); this is widely used in underwater vehicles. The disadvantage of this system is that it requires more power than the ballast system since the propeller(s) must constantly rotate in order to maintain depth. The ballast system is therefore more preferred in robotics application, since it requires less power than a propeller system in maintaining depth underwater, thus allowing longer deployment time.

In order to produce a fully deployable undulating-fin robot, a two-piston variable-density chamber as

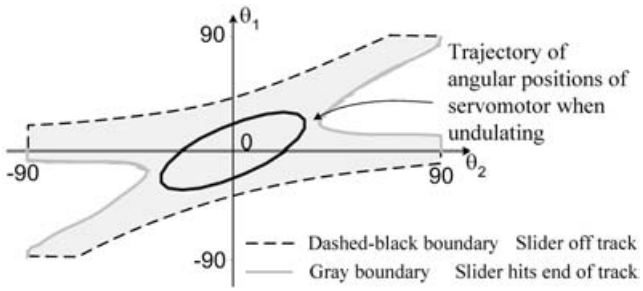

Fig. 14 Workspace of the undulating-fin mechanisms of constant-amplitude envelope and 45° phase difference β. All fin segments trace the same trajectory owing to the constant-amplitude envelope. Note that the positions of servomotors refer to points B and D in Fig. 5

a buoyancy body is designed and attached to the undulating-fin mechanism, as shown in Fig. 16.

4.1 Electronic configuration and program for buoyancy control

The simplified signal mapping for the buoyancy is shown in Fig. 17. Note that the electronic configuration for the undulating fin (see Fig. 10) is separated from the electronic configuration of the buoyancy tank with a separate power source. To demonstrate the depth-control implementation of the robotic fish, a *DepthController* program flow chart is shown in Fig. 18. The program first obtains

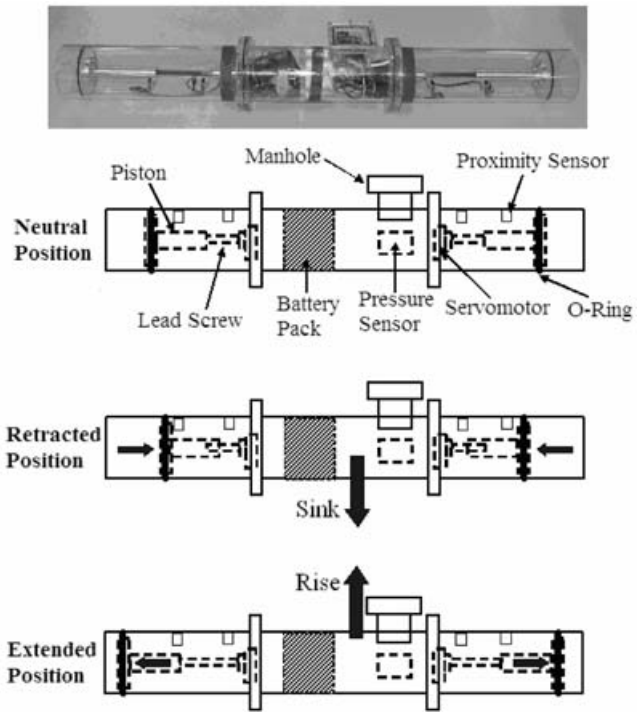

Fig. 16 A two-piston variable-density buoyancy tank attached to the fin mechanism

the actual depth and tilt angle from the depth and pitch sensors. The actual depth is then compared with the desired interval of allowable depth. If the actual depth is found to be smaller than the allowable

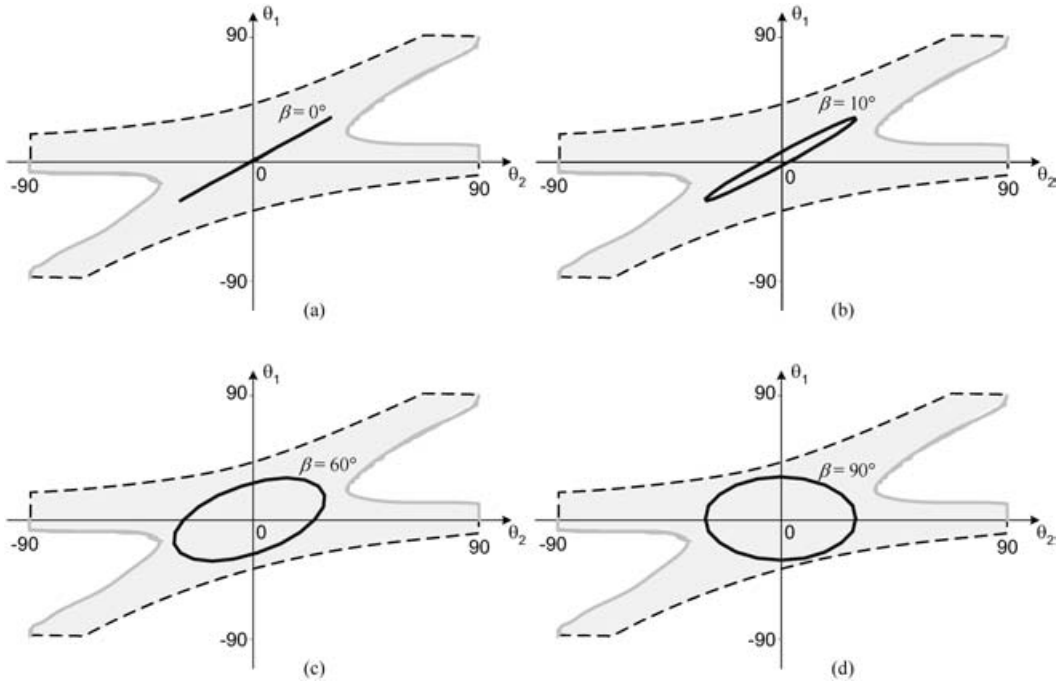

Fig. 15 Trajectories traced by undulating-fin mechanisms at various β: (a) $\beta = 0°$; (b) $\beta = 10°$; (c) $\beta = 60°$; (d) $\beta = 90°$. The size of the trajectory is proportional to the size of the amplitude envelope

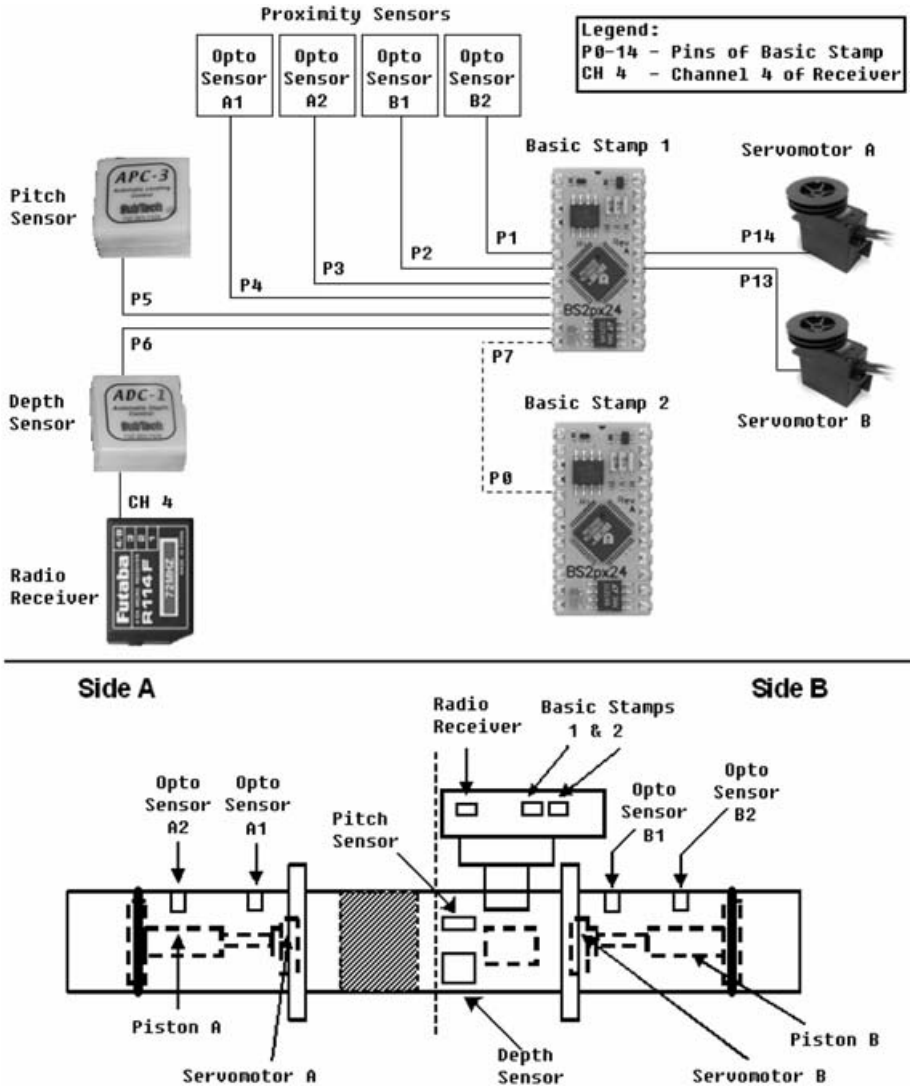

Fig. 17 Electronic configuration of the buoyancy tank

value, it means that the robotic fish is too shallow. When this happens, the program will first determine whether there is a tilt by looking at the actual tilt angle. If there is a tilt, the program will only retract the piston on the shallower side. If there is no tilt, both pistons will retract to make the robot fish go deeper. On the other hand, if the actual depth is found to be larger than the allowable value, it means that the robot is too deep. When this happens, the program will again determine whether there is a tilt by looking at the actual tilt angle, and action will be taken accordingly, as just mentioned.

The decision to extend or retract depends on the output signals from the four Opto proximity sensors, which help to determine whether any of the pistons has reached either the inner or the outer limits of the buoyancy tank.

5 EXPERIMENTS ON THE KNIFEFISH ROBOT

Using the same design and control methodology, a robotic knifefish with an anal fin has been constructed and tested. Figure 19 shows an experimental set-up to capture and measure the movement of the designed knifefish robot, whose specifications are listed in Table 1.

An important factor that must be taken into consideration when capturing an object moving at a certain frequency is the capture rate or sampling frequency. In the experiments, a video camera with a sampling frequency of 25 frames/s was used to capture the robot's motion, whose undulating frequency is set for $\frac{8}{9}$ Hz.

Figures 20 and 21 show the velocities measured and generated for eight experiments with different β.

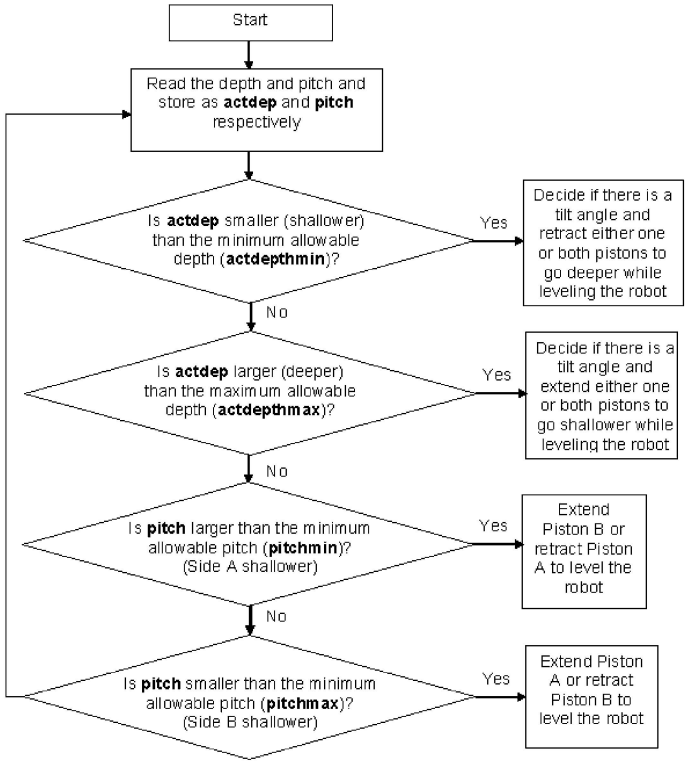

Fig. 18 *Depth_Controller* program flow chart

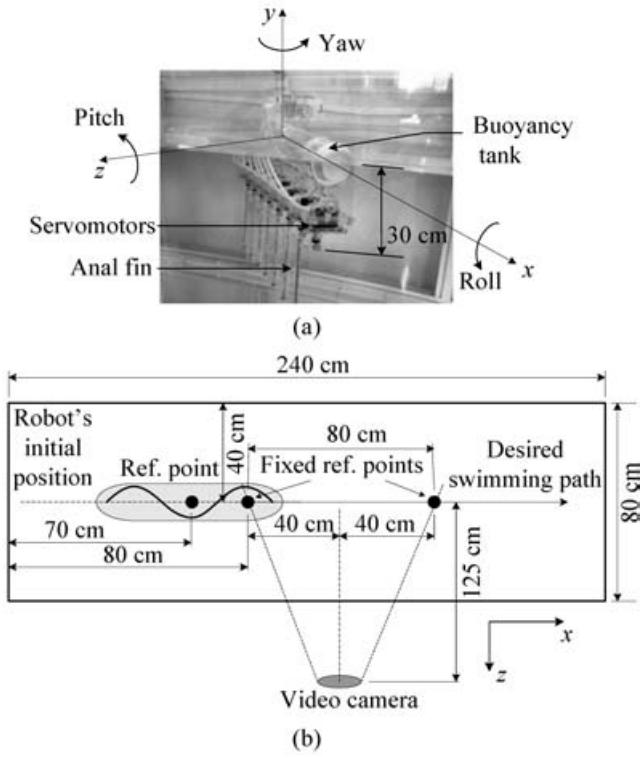

Fig. 19 Knifefish robot swimming, by an anal fin, and submerged 30 cm underwater. (b) Top view of the experimental set-up in a 240 cm × 80 cm water tank and a video camera

The four experimental results in Fig. 20 show a pattern with periodic variations. Another noteworthy observation of Fig. 20 is that the pattern repeats itself at a frequency near that of the undulating frequency, which is $\frac{8}{9}$ Hz.

Roll and yaw oscillations (see Fig. 19(a) for the definitions) were not apparent by direct observations in experiments 5 to 8 in Fig. 21. The velocity curves obtained from these experiments reveal that roll and yaw were completely absent when the robot is moving forwards. Their absence seems to confirm the analysis made by Sfakiotakis *et al.* [**17**] and Lindsey [**18**] stating that at least one wave (or cycle) is present when a fish is swimming.

Note that an undulating fin is normally characterized by the number N of waves (or cycles) presented, which is related to β (rad) by

$$N = \frac{\beta n_f}{2\pi} \tag{6}$$

where n_f is the number of fin segments connected by $n_f + 1$ servomotors ($n_f = 7$ in this case).

Figure 21 also shows the relatively constant velocity curves obtained from experiments 5 to 8. Experiments 7 and 8 show small oscillations, as the robot was gaining speed from rest. A relatively constant velocity was observed after 1 s. In other words, a

Table 1 Outline of the knifefish robot specifications

Biomimetic knifefish robot		Undulating fin	
Parameter	Value	Parameter	Value
Mass	6.2 kg	Mass	3 kg
Length	80 cm	Length	63 cm
Height	56 cm	Material	Acrylic
Width	11 cm	Width	20 cm
Actuator	8 servomotors, Futaba S3801	Peak-to-peak amplitude	10 cm
Power source	7.5 V, 3000 mA h NiMH battery	Controller	4 parallel processing Basic Stamps
		Fin segments	7 segments (8 servomotors)

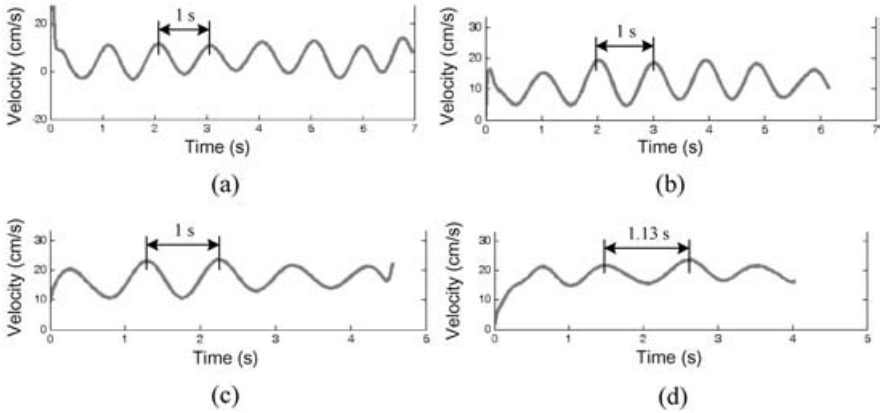

Fig. 20 Velocity of various swimming modes for $N<1$ ($\alpha=8/9$ Hz): (a) experiment 1 ($\beta=20^\circ$); (b) experiment 2 ($\beta=30^\circ$); (c) experiment 3 ($\beta=40^\circ$); (d) experiment 4 ($\beta=50^\circ$). The patterns display periodic variations

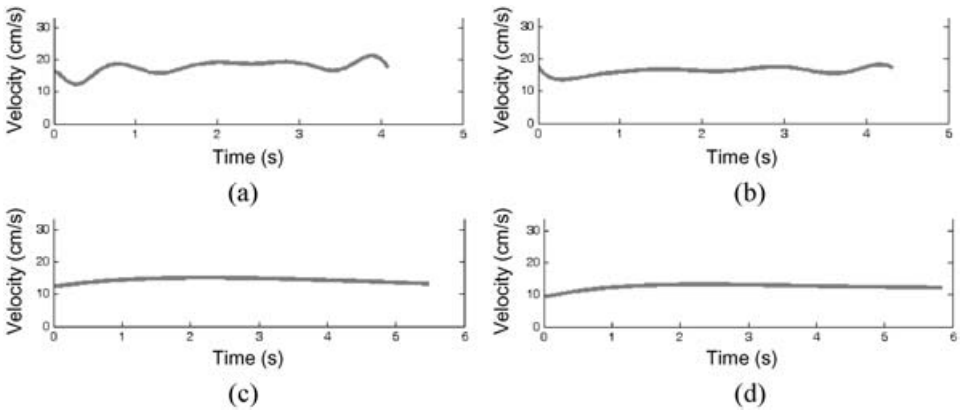

Fig. 21 Velocity curves when $N>1$ ($\alpha=8/9$ Hz): (a) experiment 5 ($\beta=60^\circ$); (b) experiment 6 ($\beta=70^\circ$); (c) experiment 7 ($\beta=80^\circ$); (d) experiment 8 ($\beta=90^\circ$). Nearly constant velocity was observed in these experiments

constant velocity and the absence of roll and yaw are desirable since the robot's swimming path can be fully controlled. Experiments 5 to 8 also showed that the robot could move in a straight line, when more than one wave ($N>1$) was present in undulations. However, the number of waves does not seem to be proportional to the increase in velocity, as shown in Fig. 22. In the white area ($N>1$), the velocity is declining, as more waves were present in undulations. The grey area shown in the figure, in which periodic velocity variations are observed, is not of interest as it only contributes to inefficient swimming [**17**, **18**]. Note that the darker area (smaller N) suggests more apparent periodic velocity variation, and roll and yaw oscillations. Figure 22 also depicts that the maximum velocity occurs near $\beta=50^\circ$, the running frequency of the motor. At this speed, no roll, yaw, and pitch were observed. With the absence of roll, yaw, and pitch, more of the input energy will be transforming to energy to drive the knifefish robot forwards.

The presence of roll and yaw can be explained by the three cases depicted in Fig. 23, in which the

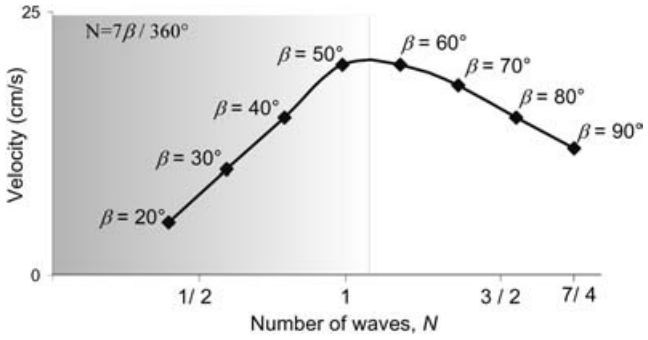

Fig. 22 Velocity of the 63 cm fin obtained from the water tank experiment ($\alpha = 8/9$ Hz). Owing to the oscillatory nature of velocity for β less than 60°, the velocity in the grey area is plotted on the basis of its time-averaged value

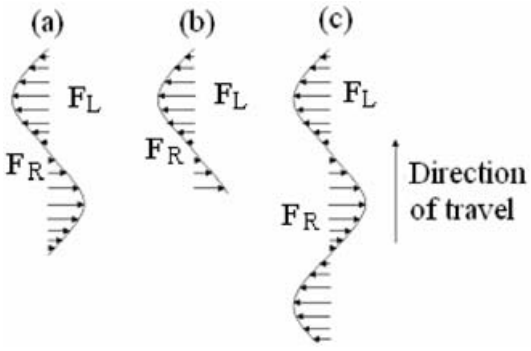

Fig. 23 Undulating-fin forces in three cases

component of force perpendicular to the direction of travel of the knifefish robot is shown.

In case (a), as the phase difference β is about 55°, the number of waves formed along the undulating fin is $N = 1$ (see Fig. 22). When this happens, the force acted by the undulating fin on the surrounding water is shown in Fig. 23(a). The force acting on the water towards the left equals the force acting on the water towards the right, i.e. $F_L = F_R$, the case of balancing.

In case (b), as the phase difference is less than 55°, the number of waves formed along the undulating fin is $N < 1$. When this happens, the force acted by the undulating fin on the surrounding water is shown in Fig. 23(b). The force acting on the water towards the left is larger than the force acting on the water towards the right, i.e. $F_L > F_R$. This causes an unbalance of force and results in the presence of roll and yaw.

In case (c), as the phase difference is more than 55°, the number of waves formed along the undulating fin is $N > 1$. Similar to case (b), there is an unbalance force with $F_L > F_R$. This again results in the presence of roll and yaw. However, the percentage of resultant unbalanced force to the balanced force in case (c) is much smaller than that in case (b). This results in much less roll and yaw (almost none).

6 CONCLUSION AND FUTURE WORK

An integrated mechanism has been developed to enable the fin rays to oscillate in arbitrary waves at a certain phase lead or lag. The integrated system consists of a buoyancy fish body attached to which is a set of flexible fins. The designed modular fin mechanism can also be redesigned better to mimic the swimming modes of fish with different fin types. Arbitrary or non-harmonic fin waves can be achieved by varying the rotation and phase difference of the servomotors. Because the fin is made of a rigid material and because of independent control of each fin ray, the application of the modular fin mechanism is not limited to oscillating fins.

A more thorough study on fin locomotion and hydrodynamics should be carried out in order to render proper and efficient control action on the current robot. An efficient force measurement of the robotic fish will be useful to the locomotion study. Therefore, future experiments should focus on how to obtain the force and the power of the undulating fins. The results enable the effective undulations for energy saving to be determined.

The future of biomimetic application relies on the advanced development of actuators. Emerging biologically inspired materials [**24–28**] such as electro-active polymer and shape-memory polymer suggest avenues worth pursuing, which may replace current motor-based actuators. These smart materials have a potential in modelling the fish muscles, including undulating fins.

Future focus will also be on data acquisition from experiments, which can then be used to analyse the deployability (feasibility for deployment) of the robotic fish. Useful areas can also include the mission execution by a school of robotic fish led by a master or parent unit. The communication and coordination among the units are especially crucial in these applications. Research methodology and technology of vehicle navigation is also crucial to the localization and recovery of robot fish in open water.

Longer battery life and more efficient communication systems are other issues before the robot fish can be implemented and adopted for useful applications in the marine and defence industries. It will also be worthwhile to explore the use of sensors that could imitate the lateral line sensory organs of fish that they use to regulate their swimming in

response to external 'disturbances'. In conclusion, the ultimate goal is to design fish-like submersible robots, which might be quieter, more manoeuvrable, and possibly more energy efficient, when compared with those submersibles using other means.

ACKNOWLEDGEMENTS

The author wishes to thank reviewers for their constructive suggestions that have greatly improved the quality of the revised version. Thanks are also due to Dr F. M. J. Nickols for his valuable assistance in the early stage of the development of the first prototype. Help given by Miss T. S. Indrawati, Mr A. Willy, and Mr W. L. Aw on the prototype development are greatly appreciated. The author would also like to acknowledge the support from Dr Gerald Seet, the Director of Robotics Research Center (RRC), and the technicians of the RRC at the water tank, electronic equipment, and other facilities.

REFERENCES

1 **Triantafyllou, M. S., Triantafyllou, G. S.,** and **Yue, D. K. P.** Hydrodynamics of fishlike swimming. *A. Rev. Fluid Mechanics*, 2000, **32**, 33–53.
2 How ships traffic noise affects whales in a shipping channel http://www.pbs.org/odyssey/odyssey/20030506_log_transcript.html, May 2003.
3 **Fish, F. E.** Limits of nature and advances of technology: what does biomimetics have to offer to aquatic robots. *Appl. Bionics and Biomechanics*, **3**(1), 2006, 49–60.
4 **Hover, F. S.** and **Triantafyllou, M. S.** Some robotic applications in fluid mechanics: vortex-induced vibrations and fish propulsion. In Proceedings of the Fluids Engineering Division, ASME Summer Meeting, Washington, DC, USA, 1998 (American Society of Mechanical Engineers, New York).
5 **Kato, N.** Locomotion by mechanical pectoral fins. *J. Mar. Sci. Technol.*, 1998, **3**, 113–121.
6 **Read, D.** *Fins for control and maneuvering of underwater vehicles.* MS Thesis, Massachusetts Institute of Technology, Cambridge, Massachusetts, 1999.
7 **Barrett, D. S., Triantafyllou, M. S., Yue, D. K. P., Grosenbaugh, M. A.,** and **Wolfgang, M.** Drag reduction in fish-like locomotion. *J. Fluid Mechanics*, 1999, **392**, 183–212.
8 **Barrett, D. S.** *Propulsive efficiency of a flexible hull underwater vehicle.* PhD Thesis, Massachusetts Institute of Technology, Cambridge, Massachusetts, 1996.
9 **Triantafyllou, M. S.** and **Triantafyllou, G. S.** An efficient swimming machine. *Sci. Am.*, 1995, **272**, 64–70.
10 **Wolfgang, M., Tolkoff, S., Techet, A., Barrett, D., Triantafyllou, M. S., Yue, D., Hover, F., Grosenbaugh, M.,** and **McGillis, W.** Drag reduction and turbulence control in swimming fish-like bodies. In Proceedings of the International Symposium on *Seawater drag reduction*, Newport, Rhode Island, USA July 1998, pp. 463–469.
11 **McHenry, M. J., Pell, C. A.,** and **Long, Jr, J. H.** Mechanical control of swimming speed: stiffness and axial wave form in undulating fish models. *J. Expl Biology*, 1995, **198**, 2293–2305.
12 **Rosenberger, L. J.** and **Westneat, M. W.** Functional morphology of undulatory pectoral fin locomotion in the stingray *Taeniura Lymma* (Chondrichthyes: Dasyatidae). *J. Expl Biology*, 1999, **202**, 3523–3539.
13 **Lauder, G. V.** and **Drucker, E. G.** Morphology and experimental hydrodynamics of fish fin control surfaces. *IEEE J. Oceanic Engng*, 2004, **29**(3), 556–571.
14 **Westneat, M. W., Thorsen, D. H., Walker, J. A.,** and **Hale, M. E.** Structure, function, and neural control of pectoral fins in fishes. *IEEE J. Oceanic Engng*, 2004, **29**(3), 674–683.
15 **Standen, E. M.** and **Lauder, G. V.** Dorsal and anal fin function in bluegill sunfish *Lepomis macrochirus*: three-dimensional kinematics during propulsion and maneuvering. *J. Expl Biology*, 2005, **208**, 2753–2763.
16 **Breder, C. M.** The locomotion of fishes. *Zoologica*, 1926, **4**, 159–297.
17 **Sfakiotakis, M., Lane, D. M.,** and **Davies, J. B. C.** Review of fish swimming modes for aquatic locomotion. *IEEE J. Oceanic Engng*, 1999, **24**, 237–252.
18 **Lindsey, C. C.** Form, function and locomotory habits in fish. In *Fish Physiology*, VII, *Locomotion* (Eds W. S. Hoar and D. J. Randall), 1978, pp. 1–100 (Academic Press, New York).
19 **Kier, W. M.** and **Thompson, J. T.** Muscle arrangement, function and specialization in recent coleoids. *Berliner Paläobiologische Abhandlungen* 03, 141–162.
20 **Low, K. H.** and **Willy, A.** Biomimetic motion planning of an undulating robotic fish fin. *J. Vib. Control*, **12**(12), 1337–1359.
21 **Willy, A.** *Design and development of undulating fin.* Master's Thesis, School of Mechanical and Aerospace Engineering, Nanyang Technological University, Singapore, 2005.
22 **Willy, A.** and **Low, K. H.** Initial experimental investigation of undulating fin. In Proceedings of the IEEE–RSJ International Conference on *Intelligent robots and systems* (*IROS2005*), Edmonton, Canada, 2005, pp. 1600–1605 (IEEE, New York).
23 **Helfman, G. S., Collette, B. B.,** and **Facey, D. E.** *The diversity of fishes*, 1999 (Blackwell Science, Oxford).
24 **Kim, B., Kim, D.-H., Jung, J.,** and **Park, J.-O.** A biomimetic undulatory tadpole robot using ionic polymer–metal composite actuators. *Smart Mater. Structs*, 2005, **14**, 1579–1585.

25 **Paquette, J. W.** and **Kim, K. J.** Ionomeric electroactive polymer artificial muscle for naval applications. *IEEE J. Oceanic Engng*, 2004, **29**, 729–737.

26 **Punning, A., Anton, M., Kruusmaa, M.,** and **Aabloo, A.** A biologically inspired ray-like underwater robot with electroactive polymer pectoral fins. In Proceedings of the IEEE International Conference on *Mechatronics and robotics* (*MechRob2004*), Aachen, 2004, Vol. 2, pp. 241–245 (IEEE, New York).

27 **Guo, S., Fukuda, T.,** and **Asaka, K.** A new type of fish-like underwater microrobot. *IEEE/ASME Trans. Mechatronics*, 2003, **8**(1), 136–141.

28 **Sfakiotakis, M., Lane, D. M.,** and **Davies, B. C.** An experimental undulating-fin device using the parallel bellows actuator. In Proceedings of the IEEE International Conference on *Robotics and automation*, Seoul, South Korea, 2001 (IEEE, New York).